

Pair Spectra and Magnetic Properties of Ni^{2+} in Double-Nitrate Crystals[†]

R. T. Dixon and J. W. Culvahouse

The University of Kansas, Lawrence, Kansas 66044

(Received 2 December 1970)

The properties of isolated Ni^{2+} ions in the two divalent sites (X and Y) of the double-nitrate crystals have been determined at 77 and 4.2 K for $\text{La}_2\text{Zn}_3(\text{NO}_3)_{12} \cdot 24\text{H}_2\text{O}$ and $\text{La}_2\text{Mg}_3(\text{NO}_3)_{12} \cdot 24\text{H}_2\text{O}$. The spectra of nearest-neighbor $X-Y$ and $X-X$ pairs have been identified and interpreted to obtain the single-ion properties of the members of the pairs and the spin-spin interactions between them. To an accuracy of 1%, the interaction between all pairs is described by the dipolar interaction plus an isotropic bilinear exchange $J\hat{S}_1 \cdot \hat{S}_2$. For nearest-neighbor $X-Y$ pairs, we find $J(X, Y) = 0.096 \pm 0.002 \text{ cm}^{-1}$ (antiferromagnetic), and for nearest-neighbor $X-X$ pairs, $J(X, X) = -0.095 \pm 0.003 \text{ cm}^{-1}$ (ferromagnetic). These results apply to both the zinc and magnesium compounds. The experimental value for $J(X, Y)$ agrees encouragingly well with the value 0.100 calculated from a model for the exchange developed earlier for Co^{2+} ions in these two sites. The measured spin-spin interaction constants for the pairs are used to predict the paramagnetic absorption spectrum of $\text{La}_2\text{Ni}_3(\text{NO}_3)_{12} \cdot 24\text{H}_2\text{O}$, which is found to agree with the experiment for only narrow ranges of zero-field splittings (D) for the X and Y ions. The spin-spin interactions and single-ion properties dictate an unambiguous choice for the ordered state of lanthanum-nickel double nitrate. It has proved possible to calculate the total ordering energy and the specific heat at temperatures well above and well below the ordering temperature 0.393 K. These detailed calculations are made possible by the fact that the zero-field splitting term for the Y ion, $D(Y)[S_z(Y)]^2$, is much larger than the spin-spin interactions, which leads to a strong suppression of the effects of the transverse part of the $X-Y$ interaction. We find that $D(Y)$ is near -2.25 cm^{-1} at all temperatures and in all double nitrates that we have investigated. The results of these calculations are in good agreement with the experimental results obtained by other investigators. The results obtained for $J(X, X)$ provide additional, but not definitive, information on exchange mechanisms for the $X-X$ pairs.

I. INTRODUCTION

In most of the classical paramagnetic salts grown from aqueous solutions, the density of magnetic ions is very low. The magnetic ions are usually clothed in a shell of water molecules and these hydrated complexes are bound to each other primarily by hydrogen bonds. Consequently, the superexchange interactions are quite weak, but still larger than the dipolar interactions. The double-nitrate crystals are typical of these materials.¹ The magnetic transition temperatures are all below 1 K even for full concentrations of divalent magnetic ions.

The development of an *ab initio* theory for the interaction of magnetic ions in such complex environments would be a formidable undertaking, and one that would be impossible without extensive information from measurements of the superhyperfine interaction with the nuclei of the ligands. It is our intention to improve our understanding of spin-spin interactions in these complex situations through the use of a semiempirical theory in which we postulate exchange potentials between electrons in symmetry-adapted d orbitals. There is reason to hope that there will be many cases in which only a few orbitals will be importantly involved in the exchange and that it may be possible to obtain a

description of many chemically different ions in the same sites with just a few parameters.

The double nitrates have two different divalent sites which we designate the X and the Y sites. Culvahouse and Schinke² used pair spectra to deduce the spin-spin interactions between Co^{2+} in nearest neighbor (NN) $X-Y$ and $X-X$ sites. They found that the degree of anisotropy in the $X-Y$ interaction could be explained quite precisely if it was assumed that only the e_g -hole orbitals were involved in the exchange between NN $X-Y$ sites. The anisotropy of the $X-X$ interaction was such that the t_{2g} orbitals must be involved in that exchange process.

In an octahedral field, the lowest orbital states of Co^{2+} are the triplet T_1 which is mostly an $e_g^2 t_{2g}$ configuration. The singlet A_2 state formed from e_g^2 is the parent of that part of T_1 which is of the $e_g^2 t_{2g}$ configuration.³ This e_g^2 state is identical to the ground state of Ni^{2+} in an octahedral field if small spin-orbit effects are ignored.³ This implies that if only e_g orbitals are involved in the exchange, there is an isotropic exchange interaction between the ionic spins of Co^{2+} and between the ionic spins of Ni^{2+} , with the exchange constant for Co^{2+} just $\frac{4}{9}$ that for Ni^{2+} .⁴ For Co^{2+} in the X and Y sites we found the isotropic ionic exchange constant to be 0.0438 cm^{-1} . In the simple model presented here we conclude that Ni^{2+} ions in the X and Y site

should experience an isotropic exchange between ionic spins

$$\mathcal{H}(\text{ex}) = K_1 \vec{S}_1 \cdot \vec{S}_2, \quad (1)$$

with $K_1 = +0.0986$. The corrections from configuration admixture in both Ni^{2+} and Co^{2+} lead to a reduction of the contribution of the orbital exchange to the isotropic part of the ionic exchange and cause it to appear as anisotropic exchange between ionic spins. These effects were shown to be quite small for Co^{2+} and are even smaller for Ni^{2+} . The precise value of the corrections depend slightly on how the exchange is distributed among the e_g orbitals. In the work on Co^{2+} it was assumed that the exchange was due to the θ orbital which pointed toward the oxygen of that water of hydration which was at the end of a chain of hydrogen bonds linking the X and Y complexes (see Fig. 11 of Ref. 2).⁵ Pursuing this model one finds that K_1 in Eq. (1) is 0.100 cm^{-1} . Other distributions of the exchange between the orbitals yield predictions intermediate between the two values quoted. The results obtained for Co^{2+} in the X and Y sites of the double nitrates thus imply that the spin-spin interaction of Ni^{2+} ions in these sites will be dipolar plus an isotropic exchange very near 0.100 cm^{-1} with very small anisotropic and biquadratic exchange.

We have undertaken the study of Ni^{2+} pair spectra in the double nitrates primarily to check the predicted value of the isotropic exchange interaction for ions in the X and Y sites. We have been able to determine the spin-spin interaction between ions in the NN X sites as well, and from this we have been able to learn more about that exchange for ions in the NN X sites. While this work was in progress, measurements of the magnetocaloric properties of LaNiN ¹ were completed at Leiden.⁶ The interpretation given to those data seemed to contradict some EPR data obtained earlier by Culvahouse,⁷ which was interpreted to show that Ni^{2+} in the Y site of the double nitrates had a zero-field splitting $D(S_z)$ ² of about -2.25 cm^{-1} in both LaMgN and LaZnN . We have obtained additional measurements which verify this result and show that a similar value for D applies for the Y ion LaNiN . We have been able to calculate a number of the magnetocaloric properties of LaNiN using only numbers determined from EPR measurements and we find good agreement with the values determined at Leiden and at higher temperatures by Fenichel and Unrine.⁸

II. SINGLE-ION PROPERTIES OF Ni^{2+} IN DOUBLE NITRATES

Both the X and Y sites have trigonal symmetry and the spin Hamiltonian may be written

$$\mathcal{H} = \mu_B \vec{H} \cdot \vec{g} \cdot \vec{S} + D(S_z^2 - \frac{2}{3}). \quad (2)$$

The g tensors for both ions are isotropic within

experimental error and very close to 2.24. The values measured for a number of different situations are given in Table I. For the X site, the value of D is small and very sensitive to temperature and diamagnetic constituents. The values of D are tabulated in Table I for a large number of situations. Some of these values have been reported previously and our values agree with earlier results.

The resonance of the Y ion has been studied much less extensively. Prior to this work, the only report of a resonance due to the Y ion was that by Culvahouse,⁷ who observed resonances in dilute double nitrates which were interpreted as the forbidden transition of a spin-1 ion with a D value of about -2.25 cm^{-1} . This was assumed to be due to Ni^{2+} in the Y site for two reasons. Firstly, the spectrum of Ni^{2+} with the small D value when observed in CeZnN showed spin-spin interactions with Ce^{3+} which corresponded to the trivalent environment of the X site. Secondly, the large D value correlated satisfactorily with the large value of $g_{\parallel} - g_{\perp}$ observed for Co^{2+} in the same site. Brice⁹ used a crystal field which reproduced the g values of Co^{2+} in the Y site to calculate the D value for Ni^{2+} in this site. The result of -4.4 cm^{-1} is in the same order of agreement with experiment as are the D values calculated for the X site by the same methods.

The measurements on the Y -ion spectrum have been repeated using a magnet capable of much higher magnetic fields than the one used by Culvahouse in Ref. 7. The measurements have been made at 37 GHz as well as in the range of 13–16 GHz. The larger magnetic field has made it possible to observe both of the allowed transitions of the Y ion over a considerable range of angles, especially in the measurements at 37 GHz. In Fig. 1, the absorption spectrum of 3% Ni in LaZnN is shown for several directions of the magnetic field for a spectrometer frequency of 13.820 GHz. The lines arising from isolated Ni^{2+} ions are identified by a code which distinguishes the complex giving rise to the absorption and the order in which the lines become visible as the magnetic field is increased and is rotated away from the direction of the symmetry axis. Since the forbidden transition of the Y ion is not visible until the field is rotated away from the direction of the symmetry axis, it has acquired the designation $Y3$ whereas the forbidden transition of the X ion is designated $X1$. It is apparent that the term forbidden transition is hardly appropriate for the line $Y3$ when the magnetic field is perpendicular to the symmetry axis, but we will continue to use this term for reasons of convenience. For the field in the direction of the symmetry axis, the line $X1$ is hardly visible, but it is very narrow and becomes

TABLE I. Spin-Hamiltonian parameters for Ni^{2+} in several double-nitrate crystals.

Crystal	Site	Situation	T(K)	$D(\text{cm}^{-1})$	g_{\parallel}	g_{\perp}
LaMgN	X	Isolated	77	0.178 \pm 0.002	2.242 \pm 0.004	2.242 \pm 0.003
LaMgN	X	Isolated	4.2	0.196 \pm 0.002	2.243 \pm 0.007	2.238 \pm 0.004
LaMgN	X	X-X pair	4.2	0.260 \pm 0.002	2.243 \pm 0.007	2.238 \pm 0.004
LaMgN	X	X-Y pair	4.2	0.153 \pm 0.003	2.243 \pm 0.007	2.238 \pm 0.004
LaZnN	X	Isolated	77	0.043 \pm 0.001	2.235 \pm 0.01	2.235 \pm 0.01
LaZnN	X	Isolated	4.2	0.063 \pm 0.002	2.235 \pm 0.004	2.236 \pm 0.007
LaZnN	X	X-X pair	4.2	0.129 \pm 0.002	2.235 \pm 0.004	2.236 \pm 0.007
LaZnN	X	X-Y pair	4.2	0.052 \pm 0.003	2.235 \pm 0.004	2.236 \pm 0.007
LaNiN	X	Concentrated	77	-0.03 \pm 0.02	2.24 \pm 0.01	2.24 \pm 0.01
LaMgN	Y	Isolated	77	-2.164 \pm 0.001	2.242 \pm 0.004	2.237 \pm 0.01
LaMgN	Y	Isolated	4.2	-2.217 \pm 0.006	2.243 \pm 0.007	2.238 \pm 0.005
LaMgN	Y	X-Y pair	4.2	-2.213 \pm 0.007	2.243 \pm 0.007	2.238 \pm 0.005
LaZnN	Y	Isolated	77	-2.212 \pm 0.01	2.235 \pm 0.01	2.236 \pm 0.01
LaZnN	Y	Isolated	4.2	-2.265 \pm 0.004	2.235 \pm 0.004	2.235 \pm 0.003
LaZnN	Y	X-Y pair	4.2	-2.260 \pm 0.005	2.235 \pm 0.004	2.235 \pm 0.003
LaNiN	Y	Concentrated	4.2	(-2.247) ^a	2.24 \pm 0.01	2.24 \pm 0.01
LaNiN	Y	Concentrated	77	-2.20 \pm 0.02	2.24 \pm 0.01	2.24 \pm 0.01

^aValue obtained using a local-field correction for the shift of the peak of the Y transition.

quite prominent in a spectrum taken with a small magnetic field modulation. This line and also Y_3 are narrow because the transition frequency is not sensitive to strain-induced changes in the zero-field splitting, which is the mechanism responsible for the width of the allowed lines. Data such as those shown in Fig. 1 have been used to obtain the isolated ion spin-Hamiltonian parameters listed in Table I. The values tabulated there for members of pairs and LaNiN have been derived from data discussed in subsequent sections. It is notable that the D values for the Y ion are hardly any different in any of the host environments and that the D values for X ions are very similar in LaNiN and LaZnN, a situation reminiscent of the behavior of the g values of Co^{2+} in the double nitrates.²

There are several unusual features of the isolated X -ion resonance which need to be understood to avoid confusion in the interpretation of the pair spectra. One of these features has led to erroneous interpretations in the past.⁶ The intensity of the forbidden transition of the X ion is appreciable even when the field is along the symmetry axis. In contrast, the intensity of the forbidden transition of the Y ion appears to vanish as the field direction approaches that of the trigonal axis, as is expected for perfect trigonal symmetry. The magnitude of the intensity of the X -ion forbidden transition and the difference in behavior for the X and Y ions appear to be completely explained by the presence of random strains which destroy the trigonal symmetry and lead to terms of the form

$$\eta(S_xS_z + S_{-}S_z + S_zS_{+} + S_zS_{-}) \quad (3)$$

in the spin Hamiltonian. When the field is along the symmetry axis, this term leads to an inten-

sity for the forbidden transition which is proportional to

$$32\left(\frac{\eta}{hv}\right)^2 \left(\frac{1}{1 - (2D/hv)^2}\right)^2. \quad (4)$$

For observations at 13 GHz, the last factor is very small for the Y ion, but much larger for the X ion. The term η is probably somewhat smaller for the Y ion because of the smaller sensitivity to strain as illustrated by the insensitivity of $D(Y)$ to temperature and diamagnetic constituents. Experimentally, we find that the intensity of the forbidden transition at 13 GHz and with the field along the symmetry axis is much larger for the LaMgN host than for LaZnN. This correlates very well with the fact that $2D$ is much closer to $h\nu$ for LaMgN than for LaZnN. In fact, the absolute intensity of the forbidden line is consistent with an rms value of η that explains the width of the allowed transitions for field directions such that a distribution of values for η make a first-order contribution to the linewidth.

The above comments on the relative intensity of the forbidden transitions of the X and Y ions with the field along the symmetry axis apply equally well to measurements at 9 GHz; but when $2D > h\nu$, as it is for Ni^{2+} in the X site of LaMgN observed at 9 GHz, the forbidden transition lies at a magnetic field between that for the two allowed transitions. Under these conditions the angular variation is somewhat unusual, since the forbidden transition and the low-field-allowed transition do not cross but simply exchange their character as the direction of the field is changed from parallel to the symmetry axis to a perpendicular direction. This behavior is illustrated by the measurements reported by Mess *et al.*⁶ Those authors inter-

preted the three lines observed at fields below 10 kG as the two allowed lines of the X -ion complex and one line of an X - X pair spectrum. There are several theoretical and experimental objections to their interpretation; but perhaps the most compelling is that the line positions as a function of angle that are given by them can be fitted satisfactorily as the allowed and forbidden transitions of a Ni^{2+} ion with $D = 0.207 \text{ cm}^{-1}$.

The unlabeled lines in Fig. 1 are lines which arise from pairs except for the two rather sharp lines than can be discerned between $X3$ and $X2$ for field directions more than 54° from the symmetry axis. We have established that these lines are not due to pairs. They disappear at 77° whereas the pair lines do not. We have found no satisfactory model which explains all of the characteristics of these lines.

III. PAIR SPECTRA

A. X - Y Pairs

A bilinear spin-spin interaction can have the general form

$$\mathcal{H}_{12} = \sum_{mm'} J_{mm'}(1, 2) T_{1m}(1) T_{1m'}(2), \quad (5)$$

in which we use the tensor operator notation defined in Ref. 2. The spatial symmetry places no restrictions on the form of (5) for an X - Y pair and there are nine constants which describe the interaction. Three of these constants correspond to the Moriya-Dzyaloshinski antisymmetric interaction.¹⁰ For an orbital singlet, this interaction is of first order in the spin-orbit interaction and can be of the order of $(g-2)$ times the isotropic exchange J . However there is a near cancellation of the contributions from the two ions¹¹ so that the final result depends upon the differences of g in the two sites and these differences are less than 0.01. This implies that the antisymmetric exchange should be less than 0.001 cm^{-1} , which is considerably less than the dipolar interaction between the ions. Since the g values for the two ions are the same, the dipolar interaction itself is symmetric. We assume that there are only six parameters in (5). In terms of the notation introduced in Ref. 2 we have

$$J_{mm'}(1, 2) = J_{mm'}(1, 2) e^{i\phi_{mm'}}, \quad (6)$$

where the independent coefficients are J_{00} , J_{11} $\times (\cos \phi_{11})$, J_{10} , J_{11} , ϕ_{10} , and ϕ_{11} .

In second order, the spin-orbit interaction leads to anisotropic exchange terms of the order of $(g-2)^2 J \approx 0.01J$ which have been called the pseudo-dipolar terms.¹² In the case of Ni^{2+} ions in the double nitrates, the magnitude of these terms is affected only very slightly by the trigonal distribution at the two sites, and the major part of such con-

tributions will reflect a cubic symmetry at each site and therefore be isotropic and require a small correction to the isotropic exchange calculated without considering the spin-orbit effect. Thus the pseudodipolar part will be far less than 1% of J . Of greater potential importance are the biquadratic spin-spin interaction terms which arise from the second-order effect of the spin-orbit interaction. These are the terms which Van Vleck has called the pseudoquadrupole interaction.¹² Again, because of the overwhelming dominance of the cubic symmetry, the major part of this interaction will be of the form $J'(\vec{S}_1 \cdot \vec{S}_2)^2$, with J' of the order of 0.001 cm^{-1} .

There are two other sources of a biquadratic interaction: terms of the fourth order in the transfer integral¹³ and the electric quadrupole moments of the ions. The transfer integral is so small for a bilinear exchange of 0.1 cm^{-1} that the fourth-order contribution will be only of the order of 10^{-6} cm^{-1} . Using the quadrupole moments given by Kana-

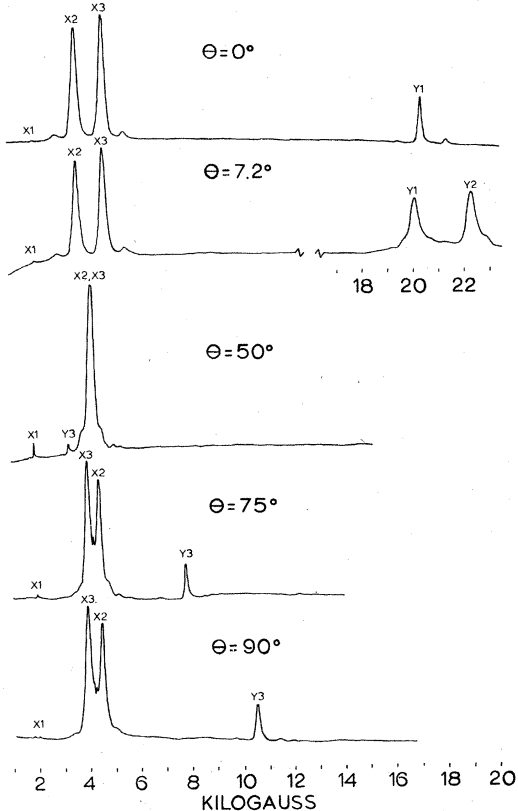


FIG. 1. Absorption spectrum of 3% Ni in LaZnN at 13.820 GHz for several directions of the magnetic field. The transitions $X1$, $X2$, and $X3$ are due to ions in the X site; and $Y1$, $Y2$, and $Y3$ are due to ions in the Y site. The numbers refer to the order in which the lines appear as the magnetic field is increased and rotated from the direction of the symmetry axis. Most of the weak lines are pair lines.

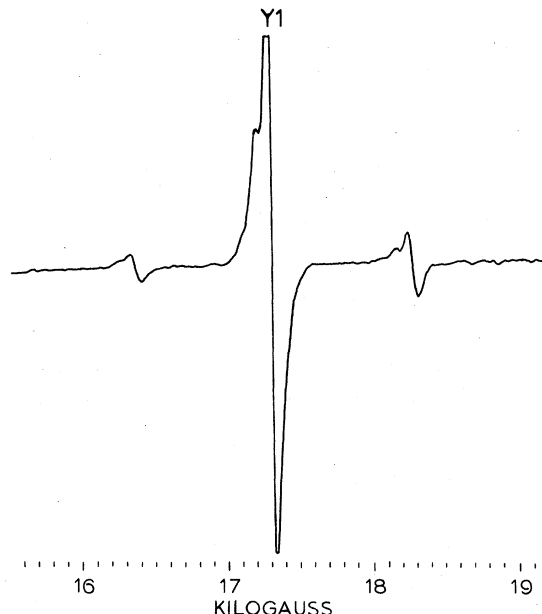


FIG. 2. Derivative of absorption near the transition Y1 with the field along the symmetry axis. The observing frequency is 13.820 GHz and the temperature is 4.2 K. The two pair lines correspond to an X-ion neighbor of the Y ion in the states $m(X) = \pm 1$. The shoulder on the resonance lines is due to twinning of this crystal.

mori,¹⁴ one finds an interaction less than 10^{-5} cm⁻¹.

In view of these estimates we attempt to interpret the pair spectra of the X-Y pairs with the symmetric form of (5). Although we expect the form to be dipole-dipole plus isotropic exchange, our approach is to use the experimental data to determine the parameters in the phenomenological form, to subtract the dipolar contributions, and to examine the character of the nondipolar part. The experimental data overdetermine some of the parameters in the bilinear interaction and we expect that the presence of biquadratic interactions will be indicated by lack of consistent agreement with experiment.

The large value of $D(Y)$ ensures that for most field directions, the transitions of the X and Y ions are separated by amounts that are large in comparison with the spin-spin interactions. In this situation, the pair spectra associated with X-ion and Y-ion transitions are well separated; and the effect of the spin-spin interaction is given to a useful approximation by a local field corresponding to the elements of \mathcal{H}_{12} that are diagonal in a product representation which diagonalizes the single-ion Hamiltonians.

The pair spectra are also affected by strain-induced changes in the single-ion Hamiltonians when the ions are members of a pair rather than

isolated. The g tensor of Ni^{2+} is extremely insensitive to strain, but there will be a symmetric quadratic spin term induced by the strain which is of the form

$$\sum_{\alpha\beta} D_{\alpha\beta} S_{\alpha} S_{\beta},$$

where the Greek subscripts refer to the coordinate axes. The effect of these terms has to be untangled from the spin-spin interaction effects.

With the field along the symmetry axis, the transition Y1 is well separated from other single-ion transitions as shown in Fig. 1. The pair lines near that transition can be discerned in Fig. 1, but the derivative spectrum in Fig. 2 shows much more detail. The slight doubling of the lines in this spectrum is caused by a twinning of the crystal. The pair spectrum consists of one line 973 G above the isolated-ion resonance and another line 935 G below. Since the Y-Y interactions were shown to be dipolar for Co^{2+} in the double nitrates, this large splitting is due to a NN X-Y pair, and is the transition of a Y ion with an X ion in one of the six NN sites. The two lines correspond to the neighboring X ion having the spin projection ± 1 along the symmetry axis. The line due to X-ion neighbors with zero-spin projection presumably lies under the isolated resonance. In first-order perturbation theory, the separation of these lines from the isolated-ion transition is given by

$$\Delta H(m) = (g\mu_B)^{-1} \{ J_{00}(X, Y)m(X) + \delta[D(Y)] \}, \quad (7)$$

where $m(X)$ is the magnetic quantum number of the neighboring X ion and $\delta[D(Y)]$ is the strain-induced change in D for the Y ion. In terms of $D_{\alpha\beta}$ we have

$$\delta[D(Y)] = D_{xx}(Y) - \frac{1}{2}[D_{xx}(Y) + D_{yy}(Y)]. \quad (8)$$

From the separation of the high- and low-field lines, one finds $J_{00}(X, Y) = 0.099$ cm⁻¹. It is apparent in Fig. 2, that the high-field pair line is more intense than the low-field line. The temperature in that case is 4.2 K, and as the temperature is lowered the upper line grows in intensity relative to the lower. This implies that $J_{00}(X, Y)$ is positive (antiferromagnetic). The dipolar contribution can be subtracted with the result $J_{00}^{(m)}(X, Y) = +0.0968$ cm⁻¹, but this is not quite precise because of second-order effects of the spin-spin interaction which affect the spacing of the $m(X) = \pm 1$ lines. These second-order effects can be estimated quite accurately by assuming that the spin-spin interaction is just dipolar plus an isotropic exchange of about 0.1 cm⁻¹. The large off-diagonal elements are primarily $\frac{1}{2}J[S_+(X)S_-(Y) + S_-(X)S_+(Y)]$. Using this we find that the low-field line $m(X) = +1$ is shifted upward by 40 G, and the high-field line $m(X) = -1$ is shifted upward by 80 G. Allowing for

this correction, we find $J_{00}^{(nd)}(X, Y) = +0.095 \text{ cm}^{-1}$.

The calculated second-order effects predict an upward shift of the center of gravity of the high- and low-field lines of 60 G. The observed shift is only 19 G. We attribute the difference to a change in $D(Y)$ for the pairs

$$\delta[D(Y)] = 0.005 \text{ cm}^{-1}.$$

These results imply that the line corresponding to $m(X) = 0$ is shifted upward by only 75 G and therefore is obscured by the isolated-ion resonance. The shoulder on the low-field side of the isolated resonance is also apparent in the pairs and is due to crystal twinning: Data taken with other crystals do not show this effect.

If one is willing to assume that the $X-Y$ interaction is really just dipolar plus isotropic exchange, the above data would be conclusive. We regard this as only a reasonably accurate determination of J_{00} subject to possible revision of the second-order correction if the transverse elements prove to be significantly different from those assumed. The other elements of (5) must be determined from

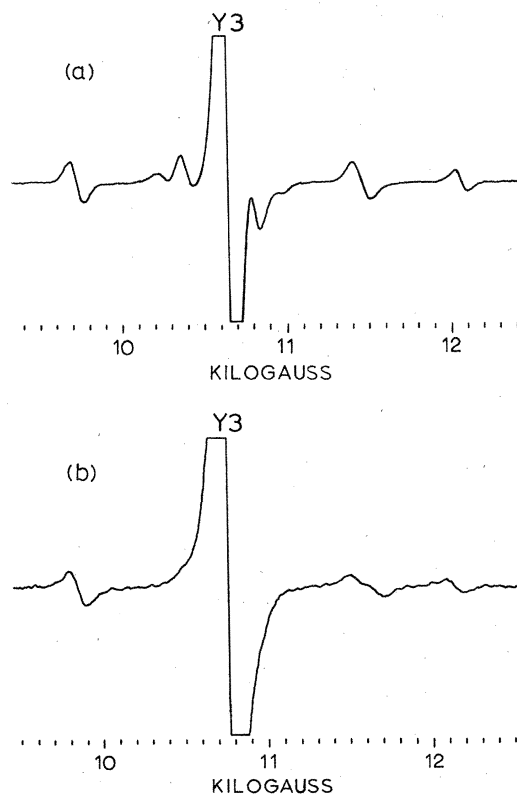


FIG. 3. (a) Derivative of absorption near the transition Y_3 with the magnetic field perpendicular to the symmetry axis for LaMgN . The frequency is 13.824 GHz and the temperature is 4.2 K. (b) Same for LaZnN at 13.845 GHz and 4.2 K. The additional lines in the LaMgN spectrum are the result of strain produced by distant neighbors.

measurements of the pair spectra in other field directions. Inspection of Fig. 1 shows that for the field in a direction perpendicular to the symmetry axis, the Y -ion transition Y_3 is well separated from all other isolated-ion transitions. For field directions in this plane, it is possible to analyze the pair spectra about the transition Y_3 with a well-organized perturbation approach. Measurements as a function of the azimuthal angle define $J_{1-1}(\cos \phi_{1-1})$, J_{11} , and ϕ_{11} .

Examples of the pair spectra about Y_3 for field directions perpendicular to the symmetry axis are given in Fig. 3. The spectrum of LaZnN shows only three resolved pair lines for the particular direction shown, but as the direction of the field is varied in the perpendicular plane, a total of nine lines can be observed. The angular variations of these nine lines are displayed in Fig. 4. The spectrum shown in Fig. 3 for LaMgN is very similar except for many extra lines near the isolated-ion transition. This complication arises from the difference in the size of the Mg and Ni ions which causes an Ni impurity to produce considerable strain. The extra lines near the isolated-ion resonance are the result of strain effects from neighbors for which the spin-spin interaction is very small. For both NaZnN and LaMgN there are three groups of three lines which we interpret to be pairs corresponding to the three values for $m(X)$ and the three types of NN sites.

With the field perpendicular to the symmetry axis, the eigenstates of the X ion for fields of the order of 10 kG are very well approximated as eigenstates of $S_{z'}$, where z' is the direction of the magnetic field. For the Y ion, it is necessary to use a representation which diagonalizes both the zero-field splitting and the Zeeman interaction. The energy eigenvalues of these states are

$$E_a = \frac{1}{2}D - \left[\frac{1}{4}D^2 + (g\mu_B H)^2 \right]^{1/2}, \quad (9a)$$

$$E_b = D, \quad (9b)$$

$$E_c = \frac{1}{2}D + \left[\frac{1}{4}D^2 + (g\mu_B H)^2 \right]^{1/2}, \quad (9c)$$

and the corresponding wave functions are

$$\Psi_a = \cos \Gamma |1, -1\rangle + \sin \Gamma |1, +1\rangle, \quad (10a)$$

$$\Psi_b = |1, 0\rangle, \quad (10b)$$

$$\Psi_c = \cos \Gamma |1, +1\rangle - \sin \Gamma |1, -1\rangle, \quad (10c)$$

where

$$\tan \Gamma = \frac{E_a - \frac{1}{2}D + g\mu_B H}{\frac{1}{2}D} \quad (11)$$

and the states $|1, m\rangle$ are eigenstates of $S_{z'}$. Transforming (5) to a set of axes defined by the field direction, we find¹⁵

$$J'_{00}(\phi, 90^\circ) = -J_{1-1} \cos \phi_{1-1} + J_{11} \cos(2\phi + \phi_{11}), \quad (12)$$

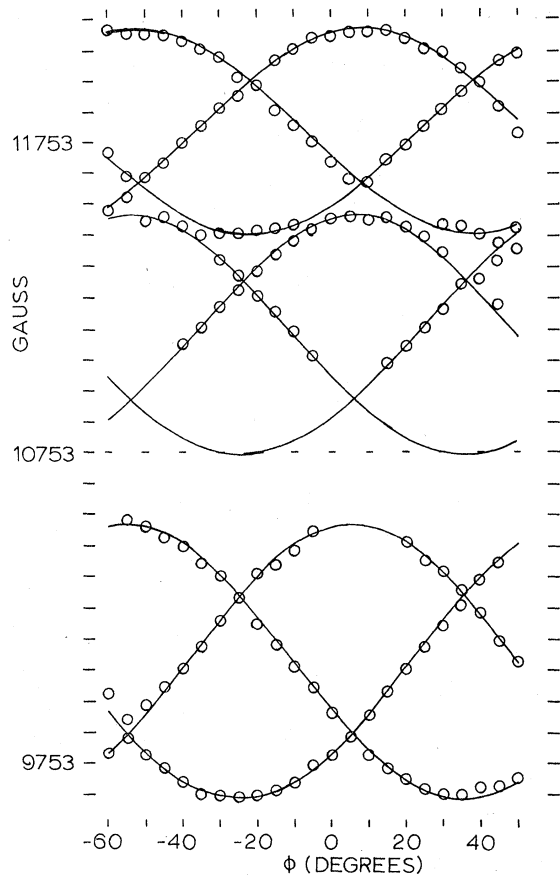


FIG. 4. Variation of the pair lines about Y_3 in LaZnN with the direction of the field in the plane perpendicular to the symmetry axis. The azimuthal angle ϕ is measured from the bisector of one of the sides of the hexagonal plate. The data were taken under the same conditions as in Fig. 3.

in which ϕ is the angle in the perpendicular plane defined by the field direction and the projection of the interionic axis $X-Y$ onto the perpendicular plane (there are therefore six distinct values ϕ and three distinct values of 2ϕ).

The transition Y_3 is between the states b and c for which it is easily verified that

$$\frac{\delta(E_b - E_c)}{\delta H} = g\mu_B \cos 2\Gamma. \quad (13)$$

We find that the first-order prediction of the field splitting from the spin-spin interaction is

$$\Delta H^{(1)}(m) = [J'_{00}(\phi, 90^\circ)/g\mu_B]m(X). \quad (14)$$

It is immediately apparent from Fig. 4, that the angular behavior of the lines is not completely described by (14). The most noticeable effect is a displacement of the $m(X) = 0$ lines and the fact that all of the lines including the $m(X) = 0$ lines show a large oscillation of nearly the same phase.

The latter effect arises from strain-induced changes in the spin-Hamiltonian of the Y ion which is no longer axially symmetric. The line positions are most sensitive to $\delta[D(Y)]$ given by (8) and the combination

$$E(Y) = \frac{1}{2} \{ [D_{xx}(Y) - D_{yy}(Y)]^2 + 4[D_{xy}(Y)]^2 \}^{1/2}. \quad (15)$$

The effect of $\delta[D(Y)]$ is independent of ϕ and calculated from the information gained from the pair spectra with the field in the direction of the symmetry axis is found to be 9 G downward. The contribution from $E(Y)$ is the same for all pair lines and is given by

$$\Delta H^{(D)}(m) = [E(Y)/g\mu_B \cos 2\Gamma] \cos \{2[\phi - \phi_E(Y)]\}, \quad (16)$$

where

$$\tan 2\phi_E(Y) = 2D_{xy}(Y)/[D_{xx}(Y) - D_{yy}(Y)]. \quad (17)$$

The introduction of this term vastly improves the description of the oscillatory part of the behavior. The amplitude of the oscillation is higher for the low-field lines than for the high-field lines, which is easily explained as a result of interference between the oscillatory parts of (14) and (16).

The large remaining discrepancy is the shift of the $m(X) = 0$ lines from a position midway between the $m(X) = \pm 1$ lines. This effect arises primarily from the second-order effects of the spin-spin interaction which we again calculate assuming that the off-diagonal spin-spin terms are given to satisfactory precision by an isotropic exchange of about 0.1 cm^{-1} . To make this calculation properly one needs to know the energy levels of the X -ion member of the pair (since this enters in the energy denominators of the perturbation result), and thus one must know the strain-induced changes in the X -ion Hamiltonian. This consideration is negligible in the calculation of the second-order effects with the field in the direction of the symmetry axis, but in the present case some of the energy denominators are only one-half wave number. The inclusion of this effect is also important because the presence of a term $E(X)$ in the X -ion Hamiltonian leads to oscillatory second-order corrections that are indistinguishable from a spin-spin interaction effect. The value of $D(X)$ can be obtained quite directly from the spectrum of the $X-Y$ pairs about the X ion with the field along the symmetry axis. The identification of these lines had to be made parallel to the analysis of the $X-X$ spectrum discussed in Sec. III B. The value of $E(X)$ was determined from a partial analysis of the $X-Y$ spectrum about the X ion with the field in the plane perpendicular to the symmetry axis. The $X-X$ pair lines and the single-ion spectra are axially symmetric so that the $X-Y$ pair lines are easily identified although frequently obscured by

TABLE II. Spin-spin interactions and strain-induced effects for $X-Y$ pairs of Ni^{2+} in LaZnN and LaMgN . The spin-spin interactions, $E(X)$ and $E(Y)$, are in units of cm^{-1} .

Quantity	Dipolar	LaZnN		LaMgN	
		Experiment	Nondipolar	Experiment	Nondipolar
J_{00}	0.0022	0.0972 ± 0.002	0.0950 ± 0.002	0.0967 ± 0.002	0.0945 ± 0.002
$J_{1-1}\cos\phi_{1-1}$	-0.0011	0.0946 ± 0.002	0.0957 ± 0.002	0.0959 ± 0.002	0.0970 ± 0.002
J_{11}	-0.0017	-0.0025 ± 0.001	-0.0008 ± 0.001	-0.0020 ± 0.001	-0.0003 ± 0.001
ϕ_{11}	0°	$3^\circ \pm 43^\circ$	$3^\circ \pm 43^\circ$	$25^\circ \pm 49^\circ$	$25^\circ \pm 49^\circ$
J_{10}		No data			
ϕ_{10}		No data			
$E(Y)$...	0.0156 ± 0.0005	...	0.0182 ± 0.004	...
$\phi_E(Y)$...	$6^\circ 50' \pm 1^\circ$...	$6^\circ 31' \pm 1^\circ 30'$...
$E(X)$...	0.0329 ± 0.003	...	0.073 ± 0.009	...
$\phi_E(X)$...	$16^\circ 26' \pm 2^\circ 30'$...	$18^\circ 31' \pm 3^\circ$...

other lines. Fortunately, the effect of the $X-Y$ spin-spin interaction is very small because at the low fields where the lines are observed the Y -ion eigenstates have a very small expectation value for S_x . We are therefore confident that most of the oscillation is due to $E(X)$ and that we can obtain a fairly reliable value from an incomplete analysis. The values which we obtained for the X -ion parameters are tabulated in Table II.

The angular variations shown in Fig. 4 were fitted to the form

$$\Delta H(m) = A_m + B_m \cos 2\phi + C_m \sin 2\phi, \quad (18)$$

with the results tabulated in Table III. The second-order effects were calculated as described in the last paragraph and the values of $J_{1-1} \cos\phi_{1-1}$, J_{11} , ϕ_{11} , $E(Y)$, and $\phi_E(Y)$ were chosen for a best fit to the experimental constants. As a further refinement, the calculations were repeated using exact diagonalization of the complete $X-Y$ Hamiltonian with the parameters obtained in the perturbation analysis. The effect of small changes in the parameters describing the Y ion and the $X-Y$ interaction was then found by perturbation theory in the representation which diagonalized the first approximation to the proper Hamiltonian. This procedure gave only very small corrections. The final values for all of the single-ion parameters and the spin-spin interaction parameters are given in Table II. The sign of $J_{1-1} \cos\phi_{1-1}$ was determined from

the temperature dependence of the relative intensity of the pair lines. The agreement of the experimental and calculated spectra can be judged by the agreement between the calculated values of the constants A_m , B_m , and C_m in Table III and the experimental values.

The nondipolar part of the $X-Y$ interaction tabulated in Table II is such that, within the experimental accuracy of about 1% or 0.001 cm^{-1} , we have

$$J_{00}^{(nd)} = -J_{1-1}^{(nd)} \cos\phi_{1-1}, \quad J_{11}^{(nd)} = 0,$$

which is expected for isotropic exchange. The best value of the isotropic exchange parameter is

$$J = \frac{1}{3}(J_{00} - 2J_{1-1}\cos\phi_{1-1}) = 0.0955 \pm 0.001 \text{ cm}^{-1}.$$

We have no information on J_{10} , J_{01} , ϕ_{10} , ϕ_{01} , and ϕ_{1-1} , but regard the measurements that we have made adequate to conclude that the interaction is isotropic exchange plus dipolar within an accuracy of 1%. There could be a bilinear interaction of the order of 0.001 cm^{-1} , which we could not have distinguished from other effects.

B. $X-X$ Pairs

The $X-X$ pairs retain axial symmetry and the spin-spin interaction is rigorously symmetric for the interchange of the two ions. The spin-spin interaction contains only two parameters J_{00} and J_{1-1} . The only other parameter required to de-

TABLE III. Parameters for fitting the angular variation of $X-Y$ pairs about the Y_3 transitions with the magnetic field perpendicular to the c axis. All units are in gauss.

	A_{-1}	A_0	A_{+1}	B_{-1}	B_0	B_{+1}	C_{-1}	C_0	C_{+1}
LaZnN									
Fit to data	1027 ± 10	364 ± 21	-691 ± 14	331 ± 9	378 ± 13	428 ± 10	93 ± 13	94 ± 16	76 ± 16
Calculated	1034	367	-683	323	377	436	96	84	82
LaMgN									
Fit to data	1021 ± 10	381 ± 9	-671 ± 7	390 ± 10	417 ± 9	464 ± 6	119 ± 15	81 ± 16	64 ± 16
Calculated	1022	377	-668	387	413	467	111	78	72

scribe the pair spectra is $D(X)$ for the members of an X - X pair.

The spin Hamiltonian for the pairs may be written

$$\mathcal{H}_{XX} = g\mu_B \vec{H} \cdot [\vec{S}(1) + \vec{S}(2)] + D(X) \{ [S_z(1) + S_z(2)]^2 - \frac{4}{3} \} + K_0 \vec{S}(1) \cdot \vec{S}(2) + [K_{zz} - 2D(X)] S_z(1) S_z(2), \quad (19)$$

where $K_0 = -J_{1-1}$ and $K_{zz} = J_{00} + J_{1-1}$. With the field along the symmetry axis, the z component of the total spin

$$S_z(T) = S_z(1) + S_z(2) \quad (20)$$

is a good quantum number. The total spin itself would be a good quantum number if $K_{zz} - 2D(X)$ were 0. This latter term admixes the states with $S_z(T) = 0$, $S(T) = 0$ and 2. It is, therefore, still quite useful to use the total spin and its z component to label the states. In terms of eigenstates ϕ_m and ψ_m of the individual spin operators $S_z(1)$ and $S_z(2)$, the eigenstates and eigenvalues of (19) are

$$|2, \pm 2\rangle = \phi_{\pm 1} \psi_{\pm 1}, \quad (21a)$$

$$E_{2, \pm 2} = \pm 2g\mu_B H + \frac{2}{3}D + K_0 + K_{zz},$$

$$|2, \pm 1\rangle = 2^{-1/2}(\phi_{\pm 1}\psi_0 + \phi_0\psi_{\pm 1}), \quad (21b)$$

$$E_{2, \pm 1} = \pm g\mu_B H - \frac{1}{3}D + K_0,$$

$$|1, \pm 1\rangle = 2^{-1/2}(\phi_{\pm 1}\psi_0 - \phi_0\psi_{\pm 1}), \quad (21c)$$

$$E_{1, \pm 1} = \pm g\mu_B H - \frac{1}{3}D - K_0,$$

$$|1, 0\rangle = 2^{-1/2}(\phi_1\psi_{-1} - \phi_{-1}\psi_1), \quad (21d)$$

$$E_{1, 0} = -\frac{1}{3}D - K_{zz} - K_0,$$

$$|a+\rangle = \cos\gamma |2, 0\rangle + \sin\gamma |0, 0\rangle, \quad (21e)$$

$$|a-\rangle = -\sin\gamma |2, 0\rangle + \cos\gamma |0, 0\rangle, \quad (21f)$$

$$E_{a\pm} = -\frac{1}{3}(K_{zz} - 2D) - \frac{1}{2}K_0 \pm [(\frac{3}{2}K_0)^2 + \frac{2}{3}(K_{zz} - 2D)^2]^{1/2},$$

where

$$\cot\gamma = (2/\sqrt{18})(K_{zz} - 2D)/(E_{a+} + \frac{2}{3}D + \frac{1}{3}K_{zz} - K_0), \quad (21g)$$

$$|2, 0\rangle = 6^{-1/2}[2\phi_0\psi_0 + (\phi_1\psi_{-1} + \phi_{-1}\psi_1)], \quad (21h)$$

$$|0, 0\rangle = 6^{-1/2}[2\phi_0\psi_0 - (\phi_1\psi_{-1} + \phi_{-1}\psi_1)]. \quad (21i)$$

The allowed transitions that are induced by a magnetic field perpendicular to the applied field are characterized by $\Delta S_z(T) = \pm 1$ and $\Delta S(T) = 0$. There are therefore transitions between $|2, \pm 1\rangle$ and the states $|a\pm\rangle$ which have intensities proportional to $\cos^2\gamma$ and $\sin^2\gamma$. If the observing frequency is larger than any of the zero-field splittings, there are four pairs of lines that can be observed with each member of a pair symmetrically located about the field $h\nu/g$.

An example of the pair spectra about the X -ion resonance is given in Fig. 5. We expect to find

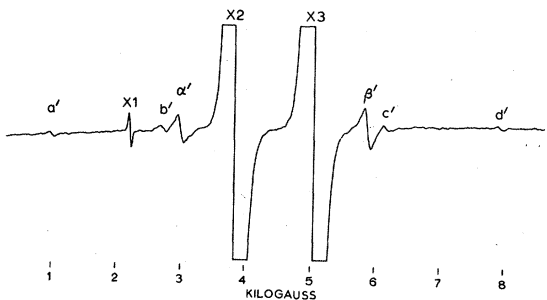


FIG. 5. Derivative of absorption near the lines $X2$ and $X3$ in LaZnN with the magnetic field in the direction of the symmetry axis. The observing frequency is 13.848 GHz, and the temperature is 4.2 K. The lines a' and b' are from X - Y pairs, the lines a' , b' , c' , and d' are from X - X pairs.

both X - X and X - Y pair lines in this spectrum. The X - Y lines must be relatively strong and occur in triads with a spacing of approximately 950 G. Further, these lines from the X - Y pairs should break up into several component lines as the direction of the magnetic field is rotated away from the direction of the symmetry axis. These criteria led to the identification of lines a' and b' in Fig. 5 as components of the X - Y pair spectra. Assuming that the other lines of the X - Y pair spectra are obscured by the isolated-ion transitions, one obtains a unique value for $D(X)$ for the X -ion member of an X - Y pair. The spectrum shown in Fig. 5 is for LaZnN. For LaMgN, more of the X - Y pair lines can be observed because of the larger spacing of the allowed transitions of the isolated X ions.

The two pairs of lines (d', d') and (b', c') are four of the possible eight lines of an X - X pair. We fitted the positions of these two pairs by the following approach: We assumed that K_{zz} has the value calculated from the dipolar interaction (that there is no anisotropic exchange), and varied both K_0 and $D(X)$ to reproduce the positions of the observed pairs with the added requirement that the other four lines had to be predicted to be unobservable. Only two solutions can be found which satisfy these criteria and they are related by inversion of the signs of both K_0 and $D(X)$. Added confidence in this interpretation was gained by repeating the analysis for LaMgN, where four X - X pair lines could again be isolated. In this case we found that the same criteria could be met with the same value of K_0 but a different value of $D(X)$.

A further test of the model and a distinction between the two choices of sign is provided by the spectrum about that of the isolated X ions with the field in the direction perpendicular to the symmetry axis, an example of which is given in Fig. 6. The lines a , b , and d exhibit axial symmetry; α and β exhibit a variation with ϕ and are

part of the spectrum of X - Y pairs. The narrow line just below $X1$ and the two sharp lines between $X1$ and $X2$ are axially symmetric lines which we do not believe to represent pairs, but for which we have found no satisfactory explanation. Accurate prediction of the field positions of the X - X pair lines for this field direction requires the exact diagonalization of the X - X pair Hamiltonian with the parameters obtained from the fit of the parallel spectrum. A good fit was found for that choice of signs which makes K_0 negative (ferromagnetic). Subtracting the dipolar contribution to K_0 we obtain $J = -0.0938 \pm 0.003 \text{ cm}^{-1}$ from the LaZnN data and $-0.0958 \pm 0.003 \text{ cm}^{-1}$ from the LaMgN data. The values of $D(X)$ are tabulated in Table I for X - X pairs in both host crystals.

As a further check on the model, the position of the pair line d' has been reproduced at angles of 10° , 20° , and 30° from the symmetry axis. The position of the line d has been reproduced for a field direction 85° from the symmetry axis. The temperature dependence of the relative intensity of the lines a' , b' , c' , and d' has been measured between 4.2 and 1.2 K and found to agree with the predictions of the model.

IV. EPR SPECTRA OF LaNiN

A. Experimental

The absorption line shape of one of the allowed lines ($Y1$) of the Y ion in LaNiN is shown in Fig. 7. The field is in the direction of the symmetry axis, the temperature is 77 K and the observing frequency is 16.204 GHz. The center position of the line corresponds to the D value tabulated in Table I. The full width at half-maximum is 4736 G and the shape is close to Gaussian. Because of the width and lack of structure, the derivative signal is very small except with very large modulation fields. We have observed the transition $Y1$ at Ni concentrations of 10% and 20% but in the latter case, there are so many overlapping pair lines that the

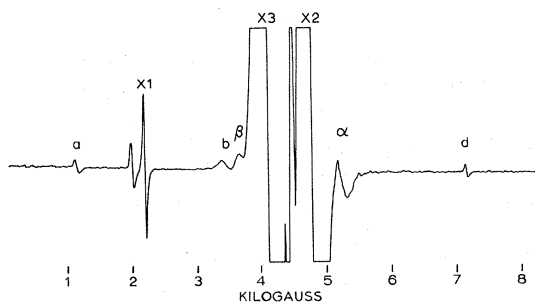


FIG. 6. Derivative of absorption near the lines $X2$ and $X3$ in LaZnN with the field perpendicular to the symmetry axis. The lines α and β are from X - Y pairs, and the lines a , b , and d are from X - X pairs. The observing frequency and temperature are the same as in Fig. 5.

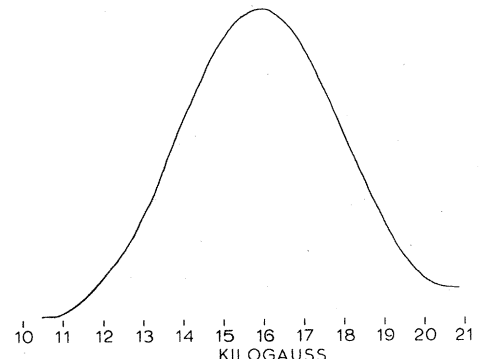


FIG. 7. Absorption due to the transition $Y1$ in LaNiN at 77 K. The observing frequency is 16.204 GHz. The full width at half-maximum is 4736 G.

observation is difficult.

The absorption spectrum of the X ions in LaNiN with the field along the symmetry axis is shown in Fig. 8(a). The peak at high field in Fig. 8(a) is the transition $Y1$. The absorption spectrum with the field perpendicular to the symmetry axis is shown in Fig. 8(b). The X -ion absorption at low fields is much more narrow than in Fig. 8(a). The line on the high-field side is due to the transition $Y3$. The X -ion absorption with the field along the symmetry axis contains considerable structure and the

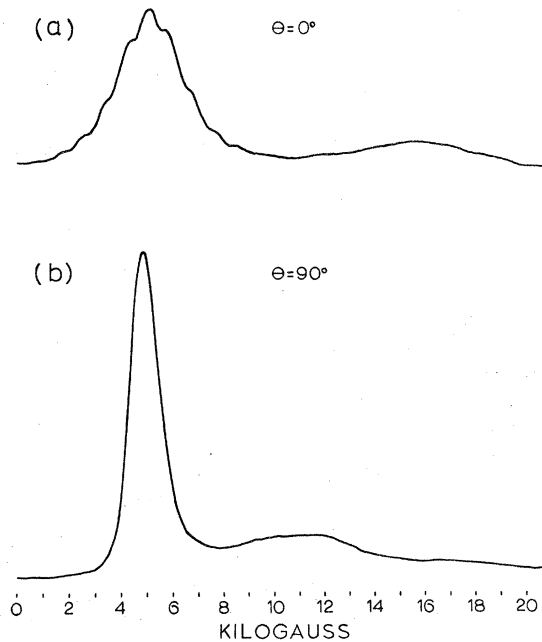


FIG. 8. Absorption spectrum of LaNiN at 77 K and for an observing frequency of 16.746 GHz with the magnetic field along the symmetry axis in (a) and perpendicular to the symmetry axis in (b). The line at high field in both spectra is due to the Y ion. The low-field absorption is due to the X ion.

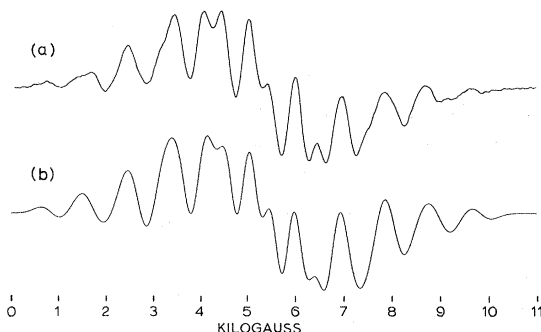


FIG. 9. (a) Derivative of absorption for the X ion in LaNiN with the magnetic field along the symmetry axis and an observing frequency of 16.742 GHz. The temperature is 77 K. (b) A calculated spectrum for the conditions corresponding to (a) and assuming spin-spin interactions between X and Y ions as those established by the pair spectra $J(X, X) = -0.094 \text{ cm}^{-1}$ and $D(X) = -0.03 \text{ cm}^{-1}$.

derivative signal is still quite strong with modulation fields of 50 G. The derivative spectrum for this field direction is reproduced in Fig. 9(a). Figure 9(b) is a calculated line shape which we discuss in Sec. IV B.

B. Calculation of Line Shapes

The calculation of the detailed line shape for the X ion in LaNiN when the field is in the direction of the symmetry axis is made possible by the large D value for the Y ion and the arrangement of the NN of an X ion. The X ion interacts strongly only with its one NN X ion and six NN Y ions. Because of the large value of $D(Y)$, the magnetic eigenstates of LaNiN crystals are well approximated by product states of the Y ion with the quantum numbers $m(Y) = \pm 1, 0$. Structurally, the X - X pairs are isolated by a shell of six Y ions with which they experience an interaction that is effectively of the Ising form $J_{00}(X, Y)S_z(X)S_z(Y)$. The transverse terms $\frac{1}{2}J_{1-1}[S_+(X)S_-(Y) + S_-(Y)S_+(X)]$, which are actually present in the interaction, are off diagonal in the representation appropriate to the Y ion, and the energy separation of the $m(Y) = \pm 1$ states from the $m(Y) = 0$ states is much larger than the spin-spin interaction for applied fields less than 18 kG. Therefore, to be a good approximation, the absorption of the X ions is that of an X - X pair interacting with the local fields produced by the six neighboring Y ions.

The local fields produced at the X sites by the Y ions are along the symmetry axis and proportional to the magnetic quantum number of the Y ion. It is convenient to consider M_A the total z component of spin for the three Y ions interacting with X -ion number 1, and the corresponding component M_B for the three Y ions interacting with X -ion number 2. The average field $[J_{00}(X, Y)(M_A + M_B)]/$

$2g\beta$ seen by the two X ions enters the Hamiltonian of the pair precisely as an applied field. However, the difference in the fields seen by the two ions (proportional to $M_A - M_B$) multiplies an X -ion operator $[S_z(1) - S_z(2)]$ which is antisymmetric for the interchange of the X ions and therefore couples the X -ion pair states with total spin $S(T) = 2, 0$ to those with $S(T) = 1$. Fortunately, $S_z(T)$ remains a good quantum number, and the magnetic field dependence of the energy levels is easily calculated once the levels have been found for zero applied field. This last problem requires the solution of numerous 9×9 determinants and requires the use of a computer. The X - Y cluster has $(3)^8$ states, but the transitions occur only between states such that there is a matrix element of $[S_z(1) + S_z(2)]$. Our procedure was to assume a set of spin-Hamiltonian parameters and to calculate the matrix elements and magnetic field position of every one of the 784 allowed transitions corresponding to an X ion. Each of these transitions was assumed to have a Gaussian shape with an rms width of 250 G and a height proportional to the square of the calculated matrix element. The derivative of these overlapping Gaussians were summed and the output displayed by a Benson-Lehner plotter.

The line shape was calculated for a number of values of $J(X, X)$ and $D(X)$ in the anticipated range, and it was soon possible to isolate features that were most sensitive to the two parameters. The final fit shown in Fig. 9(b) was obtained for $J(X, X) = -0.094 \text{ cm}^{-1}$, which is very close to the values obtained from the pair spectra. The quality of fit was fairly sensitive to $D(X)$ and the value -0.03 cm^{-1} used to obtain the result in Fig. 9(b) is precise to within 0.01 cm^{-1} . The accuracy with which $D(X)$ is determined is somewhat less than this because we have ignored small corrections from the transverse part of the X - Y interactions. These corrections would be very difficult to include in the calculation. The maximum effect on any one transition can be estimated to be about 100 G. This may account for the slightly reduced structural detail in the experimental spectrum and some of the minor errors in peak positions. We conclude that the error in $D(X)$ for LaNiN is less than 0.02 cm^{-1} and that the value of $J(X, X)$ is the same in LaNiN as in dilute crystals within 0.003 cm^{-1} .

It may be somewhat surprising that the Y -ion transition depicted in Fig. 7 displays no structure. If one just considers the local field of the 6 NN X ions, the spectrum would consist of 13 lines separated by about 950 G and with a stair-step intensity pattern from the outside to the center of the line. This result depends upon the assumption that each X ion is in a state with $m(X) = \pm 1, 0$. The calculation just made for the absorption spectrum of the X ions shows that this is not true, and the

expectation value for $m(X)$ shows a continuous range of values for the different states of an X - Y cluster.

Since the line is structureless and Gaussian in shape, we content ourselves with the calculation of the second moment by the Van Vleck method.¹⁶ The rms linewidth σ for the $Y1$ transition is given by

$$(g\mu_B)^2(\sigma^2 + H_0^2) = \text{Tr} \{ \mathcal{C}, [\sum_i S_x(i)]^2 \} / \text{Tr}(\sum_i S_x)^2, \quad (22)$$

in which H_0 is the center field for the transition $Y1$, and the $m(X) = -1$ state is understood to be omitted from the trace operation and i runs over all Y ions. The Hamiltonian is taken to be

$$\begin{aligned} \mathcal{C} = & \sum_i \{ g\mu_B H_0 S_z(i) + D(y)[S_z(i)]^2 \\ & + \sum_{\alpha i} J_{00}(i, \alpha i) S_z(i) S_z(\alpha i) \}, \end{aligned} \quad (23)$$

which includes only that part of the Hamiltonian which commutes with the total z component of spin for the Y ions and the total z component for the X ions since the inclusion of the other parts of the spin-spin interaction would include the second moment of weak satellite lines far from the main transition. The X - X interaction and the single-ion X Hamiltonian are omitted entirely since they commute with $\sum_i S_x(i)$. In (23), the index i runs over all Y ions but the index αi runs only over the NN X ions of the Y ion labeled by i . Evaluation of the traces leads to the result

$$\sigma = 2J_{00}(X, Y) / g\mu_B, \quad (24)$$

from which one finds a full width at half-maximum of 4467 G, in very good agreement with the observed value at 77 K. The result (24) is precisely the same as that calculated assuming that each X -ion neighbor produces a local field of $[J_{00}/g\mu_B]m(X)$. The calculation done this way shows that the second-order shifts apparent in the pair spectra do not contribute to the second moment and therefore not be the linewidth to the extent that the shape is accurately Gaussian.

When the Y -ion transition is observed in LaNiN at 4.2 K, the line is somewhat more narrow, asymmetrical, and shifted to higher fields. These results arise primarily from the large polarization which the X ions attain in the fields required to observe the transition. We have calculated the centroid shift due to the polarization of the X ions and obtain a value of 2256 G to higher field. This is not necessarily the same as the amount that the peak of the line is shifted; but there are more explicit line-shape models investigated by Dixon,¹⁷ which predict a most probable local field of 2518 G. When the observed field position of the peak of the Y -ion transition at 4.2 K is corrected for this local

field shift, one obtains the value for $D(Y)$ tabulated in Table I. The values of $D(Y)$ at 77 and 4.2 K show a change with temperature very similar to the changes in LaZnN and LaMgN. This gives added confidence in the model developed for the spin-spin interactions.

V. MAGNETOCALORIC PROPERTIES OF LANTHANUM-NICKEL DOUBLE NITRATE

The nature of the ordered state of LaNiN in zero field and at absolute zero is quite unambiguously determined by the measured spin-spin interactions and the single-ion properties. The ordering is dominated by the large negative value of $D(Y)$, which ensures that the Y ions will be ordered in states which are very closely eigenvalues of $S_z(Y)$ with eigenvalues ± 1 . As discussed in Sec. IV, the X - Y interaction can be treated to a good approximation as an Ising interaction. The X ions sort into X - X pairs which are in the local field of the six NN Y ions. The lowest state of the X - X pair is that with $S_z(T) = \pm 2$. The X - Y interaction energy will be minimized if the six neighboring Y ions are all ordered antiparallel to the spin of the X - X pairs. As explained in Ref. 2, the Y ions form layers perpendicular to the symmetry axis which are sandwiched between two X -ion layers 3.27 Å above and below the Y -ion layer. Each Y ion interacts with three X ions in the layer above and three in the layer below. The Y -ion layers are separated by 11.53 Å. The NN X - X pairs contribute the magnetic bonds between the sandwiches. The X - Y interaction favors an antiparallel arrangement of the X and Y layers of a sandwich, and the ferromagnetic X - X bonds favor a similar orientation for all sandwiches. The result is a ferrimagnetic structure with all of the Y ions oriented in one sense and all of the X ions in the opposite sense.

In some ways this situation is very similar to that for Co^{2+} in the double nitrates. In that case the X - Y interaction was also antiferromagnetic and highly anisotropic so that the trigonal axis was the preferred axis for the antiparallel orientation of the X and Y ions of a sandwich. The total X - X interaction was also ferromagnetic but only weakly so. The result in that case was a very delicate balance between a ferromagnetic and antiferromagnetic ordering of the sandwiches. The energy difference is so slight that the dipolar interactions between more distant neighbors appear to be the decisive factor in determining the precise nature of the long-range order. In the case of Ni^{2+} there is no ambiguity since the X - X interaction is strongly ferromagnetic and the dipolar effects are somewhat weaker than for Co^{2+} .

Assuming the ferrimagnetic ordering pattern with all X ions in one sense and all Y ions in the

opposite, the total ordering energy is easily calculated using the approximation discussed in the first paragraph of this section. There are several independent contributions. For Avagadro's number N_0 of Ni ions, the energy of the X - X pairs in their lowest energy state, ignoring X - Y interactions, is

$$U_{X-X} = \frac{1}{3}N_0\left[\frac{2}{3}D(X) + J_{00}(X, X)\right] = -0.071R.$$

The X - Y interaction is just the effect of the local field $3J_{00}(X, Y)/g\mu_B$ acting on each member of the X - X pairs and is given by

$$U_{X-Y} = -2NJ_{00}(X, Y) = -0.279R.$$

There are additional contributions from the dipolar interactions of more distant neighbors, and for a nonspherical sample there are demagnetization fields. The local dipolar field at the Y site due to more distant neighbors is 97.07 G, and the corresponding field at an X site is 51.84 G. Both fields are opposed to the direction of the moment and these interactions increase the energy of the ground state by $0.005R$ /g ion. The magnetization of the lattice at absolute zero is 16.08 G. The resulting demagnetizing fields increases the ground-state energy of a slab by $0.005R$ and decreases the ground-state energy of a long cylinder by $0.0017R$.

As a final refinement, it is not difficult to calculate the correction to the lowest energy state which arises from the transverse parts of the X - Y interaction. The large transverse terms come from the isotropic exchange and are of the form

$$\frac{1}{2}(J_{1-1} \cos \phi_{1-1})[S_+(Y)S_-(X) + S_-(Y)S_+(X)].$$

If we assume that the ground state corresponds to $S_z(Y) = +1$, then any term containing $S_-(Y)$ will have no matrix element to the ground state, and the operator $S_-(Y)$ will connect the ground state to a state in which the Y ion has been raised to the $S_z = 0$ state and thus involves considerable excitation energy.

The operators $S_-(Y)S_+(X)$ corresponding to a given Y ion and its NN X ions couple the ground state to a given excited state in which the Y ion is in the state $S_z(Y) = 0$, so that all six of the neighboring X - X pairs are in states with $M_A = 2$ and $M_B = 3$. One of the six pairs will have been raised to one of two excited states that are mixtures of $S(T) = 2$, $S_z(T) = -1$, and $S(T) = 1$, $S_z(T) = -1$. These levels are mixed together by the term $\frac{1}{2}J_{00}(X, Y)[S_z(1) - S_z(2)](M_A - M_B)$. We find that the ground state is coupled to six excited states 3.07 cm^{-1} above the ground state and six others 3.41 cm^{-1} above the ground state. Using second-order perturbation theory with $J_{1-1}(X, Y) = -0.097 \text{ cm}^{-1}$, we find that the ground state is lowered by $0.0042R$ /g ion.

The operators $S_z(Y)S_+(X)$ corresponding to a given Y ion couple to states with $M_A = M_B = 3$, and

one of the six neighboring X - X pairs in the state $S(T) = 2$, $S_z(T) = -1$ or the state $S(T) = 1$, $S_z(T) = -1$. These states lie 0.37 cm^{-1} and 0.53 cm^{-1} above the ground state, but $J_{10}(X, Y)$ is just 0.0051 cm^{-1} and the matrix elements are only 0.0036 cm^{-1} so the correction is negligible.

Adding all of these contributions we find that for a sphere, the total ordering energy is $0.711R$ /g ion. Over one-half of this arises from the zero-field splitting of the Y ion and most of the energy attributable to that source is removed by cooling to 0.7 K. The ordering energies reported by Mess *et al.*⁶ were obtained from specific-heat measurements made in the temperature range 0.12–0.7 K. In order to compare our model with their experimental results without using their extrapolation procedure we require a method for calculating

$$\Delta U = \int_{0.12}^{0.7} CdT = U - \int_0^{0.12} CdT - \int_{0.7}^{\infty} CdT, \quad (25)$$

where C is the magnetic specific heat in zero field and U is the total magnetic ordering energy. It is possible to make rather accurate calculations of the magnetic specific heat in the range below 0.12 and above 0.7 K.

In the higher-temperature range we have made a calculation of the specific heat by a method which treats the large zero-field splitting of the Y ion exactly, but is only second order in the spin-spin interactions and $D(X)$. This calculation is described in the Appendix. The result is

$$\frac{C}{R} = \frac{2[D(Y)]^2}{3(kT)^2} \frac{e^{D(Y)/kT}}{(2e^{D(Y)/kT} + 1)^2} + \frac{b(T)}{T^2}, \quad (26)$$

in which the first term represents the Schottky anomaly due to the zero-field splitting of the Y ion. The expression for $b(T)$ is given in the Appendix. The temperature dependence of $b(T)$ reflects the change in the contribution of the X - Y interaction to the specific heat as the populations of the Y -ion levels change. The temperature dependence of $b(T)$ has only minor effects between 0.7 and 4.2 K. The calculated specific heat is plotted in Fig. 10 and compared with experimental data from Refs. 6 and 8.

The integration of our analytical approximation to the specific heat from 0.7 K to infinity, yields $0.356R$ from the Schottky term and $0.052R$ from the second term. We believe that the sum of these two terms, $0.408R$, represents the prediction of our model to an accuracy of $0.005R$.

Below 0.12 K, the spin system is almost completely ordered and the specific heat can be calculated in terms of a few types of simple excitations. The low-lying excitations are those which involve flipping of X ions. The properties of the lowest-lying excitations are tabulated in Table IV. The first column contains the quantum numbers of the Y ions of the cluster and the second column the

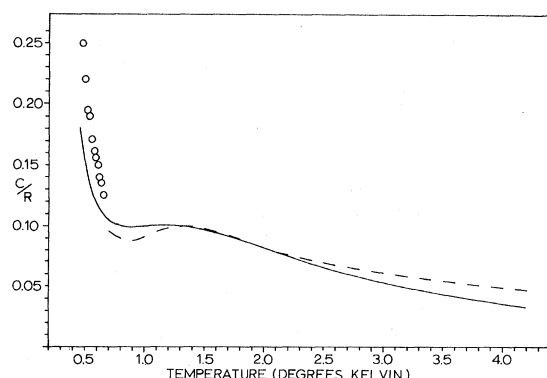


FIG. 10. Magnetic specific heat of LaNiN. The solid curve is that calculated from the EPR data. The dashed curve represents preliminary data from Ref. 8, and the open circles the data reported in Ref. 6.

quantum numbers of the X - X pairs. The fourth column contains the contribution of each excitation to the gram-ion specific heat at 0.12 K. The sum of all contributions is $0.1118R$. This does not appear to be in serious disagreement with the value of $0.15R$ reported by Mess *et al.*⁶ The fifth column of Table IV contains the contributions of each excitation to the ordering energy between 0 and 0.12 K. The total is $0.00268R$.

From these calculated results, we find $\Delta U_{\text{cal}} = 0.300R$. The corresponding experimental number can be obtained from Ref. 6, using the tabulated data and the equation $C = b/T^2$ with $b = 0.055R$ in the temperature range 0.52–0.7 K. The result is $\Delta U_{\text{exp}} = 0.304R$.

A similar calculation can be made for the entropy change between 0.12 and 0.7 K. Above 0.7 K, we find an entropy change from the Schottky term of $0.110R$, and $0.032R$ from the term $b(T)/T^2$. The total of $0.142R$ should be accurate to within $0.004R$. The total entropy change from 0 to 0.12 K is given by the sum of the last column of Table IV, $0.027R$. The total entropy from zero to infinity should be $R \ln 3 = 1.099R$. We find that the entropy change between 0.12 and 0.7 K is $0.930R$. Using the same procedure as for the energy content, we find the experimental entropy change in this temperature interval to be $0.935R$.

VI. CONCLUSIONS

We have established that J_{00} and $J_{1-1} \cos \phi_{1-1}$ correspond to the sum of the dipolar interaction and isotropic exchange with an accuracy of about 1% of the isotropic exchange for X - Y pairs and about 3% of the isotropic exchange in the case of X - X pairs. We have found that J_{11} and ϕ_{11} for the X - Y pairs is given by the dipolar interaction along to an accuracy of about 1% of the isotropic exchange. We do not have direct measurement of J_{01}, J_{10} ,

and the corresponding phase angles for the X - Y pairs, but we believe that the data presented justifies the over-all conclusion that anisotropic, anti-symmetric, and bilinear exchange between Ni ions in the double nitrates is less than 1% of the isotropic exchange. This result is in accord with theoretical expectations based on very general considerations.

We have found the ordered state that is implied by the measured spin-spin interactions and single-ion properties. The magnetothermal properties calculated with this model are in good agreement with the extensive experimental data on lanthanum-nickel double nitrate. This success as well as the EPR spectra of LaNiN verifies that the spin-spin interactions observed in pair spectra apply to the concentrated material.

The EPR spectra LaNiN shows that $D(Y)$ is about 2.25 cm^{-1} in the concentrated material. The argument against this large value which was advanced in Ref. 8 on the basis of entropy measurements appears to be incorrect because of the extrapolation procedures that were used. As stated in the last paragraph, the values calculated from the EPR measurements agree very well with the experimental results in the range where the experiments were done. The specific-heat measurements of Fenichel and Unrine⁸ in the higher-temperature ranges are in agreement with the predictions from the EPR data.

The experimentally measured isotropic exchange for Ni^{2+} ions in the X and Y sites is about 5% less than the value predicted from the Co^{2+} results. It is tempting to conclude that this reduction arises from the contraction of the e_g orbitals in Ni^{2+} relative to Co^{2+} , but we would prefer to delay such speculation until data is available for other ions in these sites. At the very least, these results suggest that the exchange between orbitals is not extremely sensitive to the ion configuration.

It was pointed out in Ref. 2 that the exchange

TABLE IV. Low-lying excitations of LaNiN and their contribution to thermodynamic properties below 0.12 K. ΔU and ΔS are the changes in the internal energy and the entropy between 0 and 0.12 K. The labels in the first two columns are the quantum numbers which define the excitation, ΔE is the excitation energy, and C/R the contribution to the specific heat at 0.12 K.

(M_A, M_B)	X-ion state	ΔE (cm^{-1})	C/R	$\Delta U/R$	$\Delta S/R$
3, 3	2, -1	0.371	0.0771	0.00208	0.02121
3, 3	1, -1	0.527	0.0238	0.00045	0.00437
3, 3	a^-	0.648	0.0085	0.00013	0.00123
3, 3	1, 0	0.854	0.0012	0.00001	0.00012
3, 3	a^+	0.866	0.0009	0.00001	0.00009
3, 3	2, 1	0.969	0.0003	0.00000	0.00002
3, 2; 2, 3	2, -2	1.164	0.0000	0.00000	0.00000

situation is much more involved for the X - X pairs than for the X - Y pairs. The anisotropy of the interaction between Co ions implies that the t_{2g} orbitals are significantly involved. The present results for Ni X - X pairs confirms this through the drastic change in the interaction for Ni ions. The nondipolar part of the interaction between Co ions is antiferromagnetic, but for Ni ions it is ferromagnetic. This implies that the exchange between two t_{2g} and/or the t_{2g} - e_g exchange is strongly antiferromagnetic while that between e_g orbitals is ferromagnetic.

One of the Goodenough-Kanmori rules summarized by Anderson¹⁸ states that ferromagnetic or potential exchange will dominate when the orbitals are in contact but orthogonal. The rule is difficult to apply when the situation is as complicated as for the X - X pairs where it is probable that the superexchange involves at least two oxygen ions. If the molecular orbitals formed from the e_g orbitals are orthogonal on the two ions, the corresponding t_{2g} orbitals may be also, and the strong antiferromagnetic exchange may arise from t_{2g} - e_g exchange. For this reason the nature of the nondipolar interaction of Co^{2+} and Ni^{2+} in NN X sites would be quite informative.

ACKNOWLEDGMENTS

The authors are grateful to Professor H. Feniche and G. Unrine of the University of Cincinnati for communication of their results on the specific heat of LaNiN in advance of publication. This investigation has profited from discussions with Professor R. C. Sapp, and one of us (R. T. D.) gratefully acknowledges support from a NASA traineeship during the initial stages of this research. Grants of computation time and the cooperation of the University of Kansas Computation Center greatly facilitated this work.

APPENDIX: SPECIFIC HEAT OF LANTHANUM-NICKEL DOUBLE NITRATE

Because of the large value of $D(Y)$ it is not possible to calculate the specific heat in the range of interest by direct expansion of $e^{-\mathcal{K}_0/\hbar T}$. We have

$$b(\tau) = \frac{4}{27} \{ [D(X)]^2 + [J_{00}(X, X)]^2 + 2[J_{1-1}(X, X)]^2 \} + \frac{4}{3} [J_{00}(X, X)]^2 (Q(\tau) \{ [D(Y)\tau]^2 + [4 + 2\gamma]D(Y)\tau + (2 + 4\gamma) \} - [Q(\tau)]^2 \{ 6[D(Y)\tau]^2 + [8 + 8\gamma + 4\gamma P(\tau)]D(Y)\tau + 8\gamma P(\tau) \} + [Q(\tau)]^3 \{ 8[D(Y)\tau]^2 + 16\gamma P(\tau)D(Y)\tau \}), \quad (\text{A11})$$

in which

$$P(\tau) = 1 - e^{-D(Y)\tau}, \quad (\text{A12})$$

[†]Work supported in part by NSF Grants Nos. GP-6701 and GP-15256. Helium gas supplied by Office of Naval Research Contract No. NOnr-2775(00).

made the calculation so that one part of the Hamiltonian,

$$\mathcal{K}_0 = D(Y) \sum_j [S_z(j)]^2, \quad (\text{A1})$$

where j runs over the Y ions, is treated exactly.

Defining

$$\mathcal{K}' = \mathcal{K} - \mathcal{K}_0, \quad (\text{A2})$$

we find that the partition function is given by¹⁹

$$Z = \left\langle e^{\mathcal{K}_0\tau} + \int_0^\tau \bar{\mathcal{K}}'(\tau_1) d\tau_1 d\tau_2 + \dots \right\rangle, \quad (\text{A3})$$

in which the angular brackets imply an ensemble average,

$$\tau = \frac{-1}{kT}, \quad (\text{A4})$$

$$\bar{\mathcal{K}}'(\tau) = e^{\mathcal{K}_0\tau} \mathcal{K}' e^{-\mathcal{K}_0\tau}. \quad (\text{A5})$$

Evaluating the traces, keeping only the first two terms in the series expansion, and omitting all but NN interactions, we find

$$Z = \langle e^{\mathcal{K}_0\tau} \rangle \{ 1 + N_Y [\omega(\tau)\tau^2 + \beta(\tau)\tau] + \dots \}, \quad (\text{A6})$$

in which the higher-order terms contain elements proportional to N_Y and to higher powers of N_Y .

The free energy is

$$F = \tau^{-1} \ln \langle e^{\mathcal{K}_0\tau} \rangle + \tau^{-1} \ln \{ 1 + N_Y [\alpha(\tau)\tau^2 + \beta(\tau)\tau] + \dots \}. \quad (\text{A7})$$

In the usual way it can be shown that in the series expansion of the logarithm, the terms proportional to powers of N_Y greater than 1 cancel so that the approximation $\ln(1+x) \approx x$ depends only on the smallness of $\alpha(\tau)\tau^2$ and $\beta(\tau)\tau$. These terms are of the order of $(\mathcal{K}'\tau)^2$, $(\mathcal{K}'')^2/\tau$, $[\mathcal{K}'/D(Y)]^2$, and $[\mathcal{K}'/D(Y)]^2$.

Using

$$\frac{C}{R} = \frac{\tau^3}{(N_X + N_Y)} \left(\frac{\partial^2 F}{\partial \tau^2} + 2\tau \frac{\partial F}{\partial \tau} \right), \quad (\text{A8})$$

we find

$$\frac{C}{R} = \frac{2}{3} [D(Y)\tau Q(\tau)]^2 e^{-D(Y)\tau} + b(\tau)\tau^2, \quad (\text{A9})$$

where

$$Q(\tau) = (2e^{D(Y)\tau} + 1)^{-1} e^{D(Y)\tau}, \quad (\text{A10})$$

$$\gamma = [J_{1-1}(X, Y)/J_{00}(X, Y)]^2 \quad (\text{A13})$$

¹The general chemical formula for the double nitrates is $[M(\text{NO}_3)_2][M'(\text{NO}_3)_3 \cdot 6\text{H}_2\text{O}]_3 \cdot 6\text{H}_2\text{O}$, where M is a trivalent rare-earth ion and M' is a divalent iron-group ion. We use the

abbreviated notation $MM'N$ with the chemical symbol for the elements M and M' .

²J. W. Culvahouse and David P. Schinke, *Phys. Rev.* **187**, 671 (1969).

³J. S. Griffith, *The Theory of Transition Metal Ions* (Cambridge U.P., London, 1961), pp. 347-348.

⁴This result follows from a discussion of exchange interaction in the excellent review by J. Owen and J. H. M. Thornley, *Rept. Progr. Phys.* **29**, 675 (1966). Because of the isotropic exchange between the ionic spins of Co^{2+} we assume that f_{π}^2 is negligible.

⁵Equation (61) of Ref. 2 is used in the calculation of this result. The numerical factor 0.94 in that equation should be 0.97.

⁶K. W. Mess, E. Lagendijk, N. J. Zimmerman, A. J. Van Duyneveldt, J. J. Giesen, and W. J. Huiskamp, *Physica* **43**, 165 (1969).

⁷J. W. Culvahouse, *J. Chem. Phys.* **36**, 1710 (1962).

⁸H. Fenichel and G. Unrine (private communication).

⁹D. K. Brice, doctoral dissertation, University of Kansas, 1962 (unpublished).

¹⁰I. Dzyaloshinski, *Phys. Chem. Solids* **4**, 241 (1958); T. Moriya, *Phys. Rev.* **117**, 635 (1960).

¹¹J. H. Van Vleck, *Phys. Rev.* **52**, 1178 (1937).

¹²Toru Moriya, in *Magnetism*, edited by George T. Rado and Harry Suhl (Academic, New York, 1963), Vol. I, pp. 92ff.

¹³P. W. Anderson, in Ref. 12, p. 41.

¹⁴Junjiro Kanamori, in Ref. 12, pp. 161-164.

¹⁵See Ref. 2, Eq. (27).

¹⁶J. H. Van Vleck, *Phys. Rev.* **74**, 1168 (1948).

¹⁷R. T. Dixon, doctoral dissertation, University of Kansas, 1970 (unpublished).

¹⁸P. W. Anderson, in Ref. 12, p. 67.

¹⁹A. Simon, M. E. Rose, and J. M. Jauch, *Phys. Rev.* **84**, 1155 (1951).

Electron States in Ferromagnetic Iron. II. Wave-Function Properties*

K. J. Duff

*Theoretical Sciences Department, Scientific Research Staff,
Ford Motor Company, Dearborn, Michigan 48121*

and

T. P. Das

*Physics Department, University of Utah, Salt Lake City, Utah 94112
(Received 7 August 1970)*

The wave functions produced by a new band calculation for ferromagnetic iron are examined by computing from them charge and spin densities both at the nuclear position and at other positions throughout the unit cell. Excellent agreement is achieved between the measurable experimental and theoretical quantities, namely, charge and spin densities, the isomer shift, and the hyperfine field. It is shown that the earlier interpretation of neutron-diffraction data and the pressure dependence of the hyperfine field in favor of a negative polarization of the $4s$ states is not soundly based. From our consideration of the band contribution to the hyperfine field, the $4s$ electrons are found to be positively polarized.

I. INTRODUCTION

It is unquestioned that the ferromagnetism of transition metals reflects an unequal spin population of the bands derived from atomic $3d$ states. Naively, one would expect that the bands derived from atomic $4s$ states would be polarized by the exchange interaction with the d states to give a net $4s$ moment parallel to the $3d$ moment. To this simple picture we have to add the effects of hybridization of s and d states which add an antiparallel component of polarization to the s bands,¹ and the resulting moment can be either positively (parallel) or negatively (antiparallel) polarized. Experimentally, evidence has been found that has been interpreted to mean that the $4s$ states of iron, cobalt, and nickel are actually polarized negatively.²⁻⁴ In this paper we consider the properties of the wave functions of conduction electrons in ferromagnetic

iron as derived in a new band-structure calculation described in a previous paper,⁵ with particular emphasis on magnetic properties. We reexamine the question of the polarization of the $4s$ electrons and conclude that they are positively polarized.

The evidence cited for negative polarization is threefold: (a) the angular distribution for the scattering of polarized neutrons²; (b) the pressure dependence of the hyperfine field³; (c) the angular correlation of γ rays from the annihilation of polarized positrons.⁴ We do not consider here (c); however, the interpretation of the positron-annihilation experiments in favor of a negative $4s$ polarization has largely been discredited⁶; it is accepted that for some momenta there is a negative polarization in iron and nickel, but it has not been possible, so far, to derive a net polarization integrated over all momenta.⁷

We must emphasize at this point that we do not